Excited-State Intramolecular Proton Transfer in a Dendritic Macromolecular System: Poly(aryl ether) Dendrimers with Phototautomerizable Quinoline Core

Sehoon Kim, Dong Wook Chang, and Soo Young Park*

School of Materials Science and Engineering, Seoul National University, ENG 445, San 56-1, Shillim-dong, Kwanak-ku, Seoul 151-744, Korea

Hideki Kawai and Toshihiko Nagamura

Research Institute of Electronics, Shizuoka University, 3-5-1 Johoku, Hamamatsu 432-8011, Shizuoka, Japan

Received August 2, 2001; Revised Manuscript Received December 11, 2001

ABSTRACT: Poly(aryl ether) dendrimers of three different generations (n = 1, 2, 3) that are cored with phototautomerizable quinoline (QGn) were synthesized to investigate the effect of dendritic architecture on the excited-state intramolecular proton transfer (ESIPT). It was deduced from the generation-dependent absorption spectra that the peripheral crowdedness arising from the dendritic structure not only decouples the ESIPT core from the molecular surrounding but also influences the core planarity. Static and picosecond kinetic studies on ESIPT emission provided further information that the ESIPT in the quinoline core is slowed down with increasing dendrimer generation via the reduced core planarity. However, it was also observed that the proton transfer is still so effective even in the highest generation dendrimer that the emission efficiency is largely increased with dendrimer generation through the enhanced isolation effect. Compared to the polystyrene blend film containing nondendritic model compound (MQ), the films of QGn were proven to be a truly single-component "solid solution" with better performances in terms of the emission efficiency and chromophore content.

Introduction

Excited-state intramolecular proton transfer (ESIPT), a phototautomerization occurring in the excited states of the heterocyclic molecules possessing a cyclic intramolecular hydrogen bond (H-bond), has been the research subject intensively studied in photochemistry and photophysics.[1−6] ESIPT-exhibiting molecules exist exclusively as enol form tautomers in the ground state, but once excited, they are preferentially transformed into the excited-state keto tautomers via an extremely fast and irreversible ESIPT process occurring in the subpicosecond time regime. After the excited keto forms decay radiatively to the ground-state keto forms, the energy-wasting backward proton transfer occurs very readily restoring their initial enol forms, which is in general very efficient and thus has been applied to UV photostabilization.[7] Moreover, the different dominant species in the ground and the excited states via ESIPT give rise to a large Stokes shifted fluorescence without self-reabsorption and also to a population inversion of the proton-transferred keto form in the lowest excited state facilitating stimulated emission. This peculiar characteristic has encouraged more novel applications such as luminescent solar concentrator[8] and proton-transfer laser.[9−12]

Despite these advantages, application of ESIPT has largely been limited by the low efficiency and prominent concentration quenching of keto emission.[13] Accordingly, most of ESIPT phenomena have been investigated rather academically in a dilute solution system, such as fluorescence probe for molecular environment. Although several polymeric systems including simple blends or copolymers have been studied academically[14] or with an aim to realize solid lasers[9,11,12,15] or electroluminescence,[11] the tolerable contents of ESIPT−chromophore were far too low in order to achieve an aggregation-free and highly efficient solid solution in a polymeric matrix. Very recently, however, we were able to synthesize an extremely concentrated but still ESIPT-active solid film consisting solely of a semirigid polyquinoline (PQH). We have already reported ESIPT kinetics of PQH and its applicability to electroluminescence.[16] PQH has two alternating structural units based on the quinoline ring as shown in Chart 1, one of which with the hydroxyl group is a novel ESIPT chromophore responsible for the abnormally large Stokes shift. Photophysical and photochemical processes related to this ESIPT chromophore are depicted for the simplified quinoline structure in Chart 2.

Chart 1. Semirigid Polyquinoline (PQH) Exhibiting ESIPT

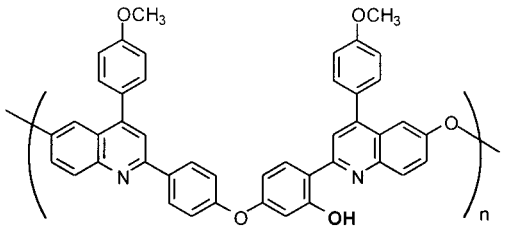

As an extension of this work, we report, in the present paper, a novel class of solid medium for ESIPT, i.e., dendrimers covalently encapsulating the same quinoline-based chromophore as in PQH. This dendritic encapsulation strategy has successfully been applied as a new methodology to alter properties of various functional chromophores.[17−24] Fréchet's archetypal poly(aryl

* Corresponding author. E-mail parksy@plaza.snu.ac.kr.

10.1021/ma011385o CCC: $22.00
Published on Web 02/19/2002

Chart 2. Photophysical and Photochemical Processes of Phototautomerizable Quinoline Compound

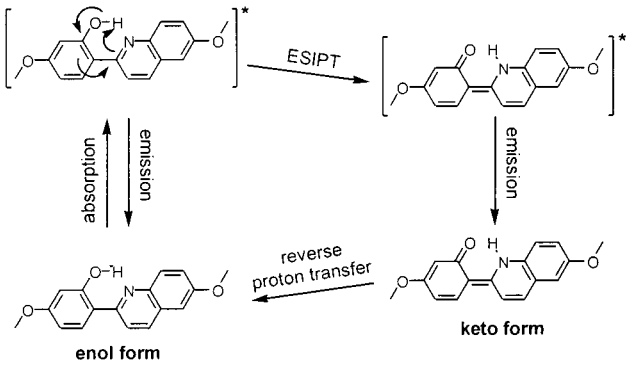

ether) dendron was chosen to suppress the concentration quenching of keto emission in the film state by spatial isolation of ESIPT chromophore. A covalently bonded and highly branched framework of the dendrimer is also expected to provide multichannel paths for the dissipation of heat generated in the core unit during the high-power lasing experiment.[12] Therefore, we propose a "ESIPT dendrimer" as a promising solid lasing material in the form of a single-component "solid solution" with a large amount of active chromophore. Herein are described the synthesis and also the static optical properties of ESIPT dendrimers together with the fluorescence kinetics.

Experimental Section

Materials. 18-Crown-6 (>99.5%), benzyl bromide (98%), methyl 3,5-dihydroxybenzoate (97%), 2′-hydroxy-4′-methoxyacetophenone (99%), 2′,4′-dihydroxyacetophenone (99%), P_2O_5 (98+%), and *m*-cresol (99%) were purchased from the Aldrich Chemical Co. All reagents were used without further purification.

Measurements. Chemical structures were identified by ^{1}H NMR (JEOL JNM-LA300, 300 MHz) and IR (Midac FT-IR spectrophotometer) spectroscopy. Mass spectra were measured by GC/mass in EI mode (JMS AX505WA) and matrix-assisted laser desorption/ionization time-of-flight (MALDI-TOF) mass spectrometry (PerSeptive Biosystem Voyager-DE spectrometer) using 1,8-dihydroxy-9[10*H*]-anthracenone in THF as a matrix. Thermal analysis was performed on Perkin-Elmer DSC7 at a rate of 20 °C/min. For the film state optical measurements, QG*n* films and polystyrene−MQ blend films with a thickness of 80−120 nm were prepared onto a glass substrate by spin-casting from the chlorobenzene solution of appropriate concentrations (3−10 wt %).

Absorption spectra were recorded on a HP 8452A diode array spectrophotometer. Emission spectra were obtained on a fluorescence spectrophotometer (Hitachi, F-4500) under the identical conditions of excitation power and measurement geometry for all the samples. Emission spectra were corrected for the optical density variation (i.e., film thickness and dye concentration) to give relative intensity by dividing absolute emission intensity with absorbance at the excitation wavelength.

Fluorescence kinetic profiles for the emission above 550 nm passed through a cutoff filter were measured using an imaging spectrograph (Hamamatsu, C5094) and a streak scope (Hamamatsu, C2830) with a high-speed streak unit (Hamamatsu, M2547). Samples were excited with the third harmonic (355 nm) of passively/actively mode-locked Nd:YAG laser (B.M. Industries, 5022 D.PS. DP10) with the pulse duration of 33 ps.

Semiempirical Calculation Method. The ground-state geometry of the simplified model structure of ESIPT chromophore (Figure 3b) was optimized using the PM3 parameter implemented in the Mopac 97 program (Fujitsu). Starting from this optimized geometry, planarity-dependent transition energies and oscillator strengths between singlet states were calculated by increasing the torsional angle (θ) around the bond connecting quinoline and phenol units by 10° with the configuration interaction calculation (90 configurations), utilizing the HyperChem 5.0 program (Hypercube).

Synthesis. Bis(aminoketone) (**1**) is a known material and was prepared following a literature method.[16] The synthesis of Fréchet's dendrons G*n*-Br (number of generation, $n = 1-3$) followed the literature procedures.[25,26] First, methyl 3,5-dihydroxybenzoate was coupled with benzyl bromide in the presence of anhydrous K_2CO_3 and 18-crown-6. The obtained methyl ester was reduced to benzyl alcohol by $LiAlH_4$ and finally converted to G1-Br in the presence of CBr_4 and PPh_3. The higher generation G2-Br and G3-Br were obtained in a similar manner starting from the coupling of methyl 3,5-dihydroxybenzoate with G1-Br and G2-Br, respectively.

Model Compound (MQ). 1.8 g of P_2O_5 was added to 3.6 mL of *m*-cresol at room temperature. The mixture was then heated to 140 °C and stirred for 2 h. After cooling, 0.1 g of bis(aminoketone) (**1**) and 0.07 g of 2′-hydroxy-4′-methoxyacetophenone (**2-OCH$_3$**) were added and stirred overnight at 140 °C. The cooled reaction mixture was poured into excess methanol, and the precipitate was collected by filtration. The filtered product was purified by column chromatography on silica gel, eluting with ethyl acetate/*n*-hexane (volume ratio increasing from 1/2 to 1/1), to afford a yellow solid (0.047 g, 30% yield); mp 98 °C. ^{1}H NMR ($CDCl_3$, ppm): 3.84 (s, 6H), 3.87 (s, 6H), 6.51 (dd, $J = 8.79$, 2.66 Hz, 2H), 6.60 (d, $J = 2.66$ Hz, 2H), 7.00 (d, $J = 8.79$ Hz, 4H), 7.40−7.50 (m, 8H), 7.82 (s, 2H), 7.84 (d, $J = 8.79$ Hz, 2H), 8.02 (d, $J = 9.15$ Hz, 2H). *m*/*z* (EI) calcd for $C_{46}H_{36}N_2O_7$, 728.79; found, 728.

Quinoline Core (3). Reaction of bis(aminoketone) (**1**, 0.59 g) and 2′,4′-dihydroxyacetophenone (**2-OH**, 0.38 g) by the procedure described above gave **3**. The crude product was purified by silica gel column chromatography with the eluent of ethyl acetate/*n*-hexane (the volume ratio increasing from 1/1 to 2/1), affording an orange solid (0.42 g, 48% yield); mp 83 °C. ^{1}H NMR ($CDCl_3$, ppm): 3.83 (s, 6H), 6.46 (dd, $J = 8.25$, 2.01 Hz, 2H), 6.54 (d, $J = 2.01$ Hz, 2H), 7.00 (d, $J = 8.22$ Hz, 4H), 7.40−7.48 (m, 8H), 7.80 (s, 2H), 7.82 (d, $J = 8.25$ Hz, 2H), 8.01 (d, $J = 9.33$ Hz, 2H). *m*/*z* (EI) calcd for $C_{44}H_{32}N_2O_7$, 700.73; found, 700.

General Procedure for Coupling of Quinoline Core (3) with G*n*-Br (QG*n*). To a solution of **3** (1 equiv) and dendritic benzyl bromide G*n*-Br (2.1 equiv) in dry acetone or THF was added 3 equiv of K_2CO_3 and 0.2 equiv of 18-crown-6. After 1 day of reflux, the reaction mixture was cooled to room temperature and diluted with excess CH_2Cl_2. The solution was then filtered, and the solvent was removed under reduced pressure. The crude product was thoroughly purified by column chromatography on silica gel to give an orange glass.

QG1 and QG1-t. 3 (0.1 g) and G1-Br (0.12 g) were coupled following the general procedure described above in acetone. Column chromatography was carried out eluting with ethyl acetate/*n*-hexane/CH_2Cl_2 (1/10/12), and the gather of the second band gave QG1 (52 mg, 28% yield). The third band was then collected eluting with ethyl acetate/*n*-hexane/CH_2Cl_2 (1/6/12) to give QG1-t (43 mg, 19% yield).

QG1. T_g 105 °C. ^{1}H NMR ($CDCl_3$, ppm): 3.84 (s, 6H), 5.05 (s, 8H), 5.07 (s, 4H), 6.56−6.61 (m, 4H), 6.67 (d, $J = 2.01$, 2H), 6.71 (d, $J = 2.19$, 4H), 7.00 (d, $J = 8.61$, 4H), 7.26−7.49 (m, 28H), 7.82−7.86 (m, 4H), 8.03 (d, $J = 8.97$, 2H). *m*/*z* (MALDI) calcd, 1305.47; found, 1303.21.

QG1-t. T_g 56.7 °C. ^{1}H NMR ($CDCl_3$, ppm): 3.81 (s, 6H), 5.02−5.05 (m, 24H), 6.56−6.82 (m, 13H), 6.98 (d, $J = 8.61$, 4H), 7.25−7.51 (m, 38H), 7.80−8.01 (m, 6H). *m*/*z* (MALDI) calcd, 1607.83; found, 1605.33.

QG2. The reaction between **3** (0.1 g) and G2-Br (0.25 g) following the general procedure was performed in acetone. The product was isolated by column chromatography using ethyl acetate/*n*-hexane/CH_2Cl_2 (1/10/12) as the eluent, to afford QG2 (0.18 g, 59% yield). T_g 53.6 °C. ^{1}H NMR ($CDCl_3$, ppm): 3.83 (s, 6H), 4.93−5.13 (m, 28H), 6.55−6.74 (m, 22H), 7.00 (d, $J =$

Scheme 1. Synthesis of Low Molar Mass Quinolines (3, MQ) and Dendritic Molecules (QG*n*)

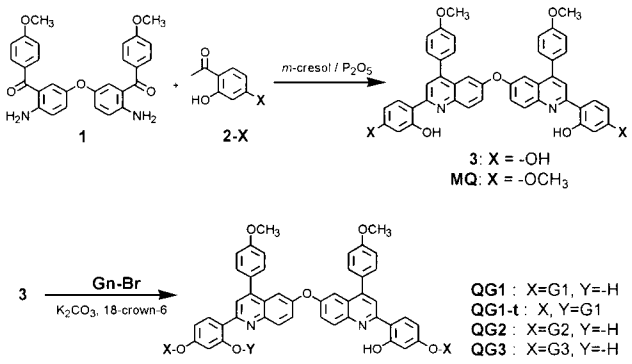

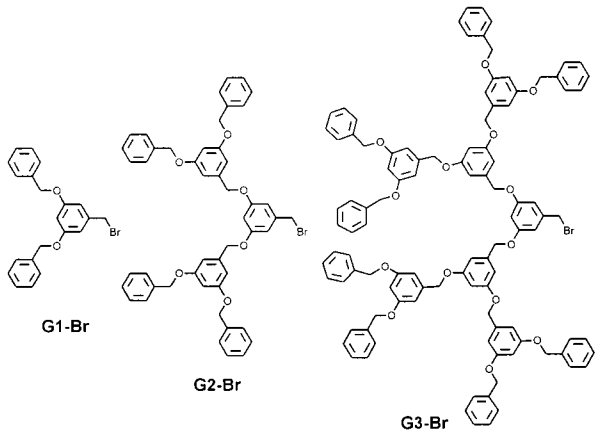

8.61, 4H), 7.26−7.49 (m, 48H), 7.78−7.82 (m, 4H), 8.01 (d, J = 8.97, 2H). *m*/*z* (MALDI) calcd, 2154.44; found, 2152.51.

QG3. The coupling reaction between **3** (0.028 g) and G3-Br (0.14 g) was performed in THF. The product was isolated by column chromatography using ethyl acetate/*n*-hexane/CH_2Cl_2 (1/10/12) as the eluent, to afford QG3 (0.12 g, 77% yield). T_g 49.7 °C. ^{1}H NMR ($CDCl_3$, ppm): 3.80 (s, 6H), 4.89−5.05 (m, 60H), 6.51−6.69 (m, 46H), 6.97 (d, J = 8.61, 4H), 7.24−7.41 (m, 88H), 7.74−7.79 (m, 4H), 7.97 (d, J = 8.97, 2H). *m*/*z* (MALDI) calcd, 3852.39; found, 3848.41.

Results and Discussion

Synthesis of Dendritic Molecules. Synthetic routes of low molar mass quinolines (**3**, MQ) and dendritic molecules (QG*n*) are depicted in Scheme 1. Benzyl bromide-focused aryl ether dendrons (G*n*-Br) are well-known compounds in dendrimer chemistry and were prepared by convergent strategy according to the literature procedures.[25,26] The dendron synthesis was well confirmed by comparable NMR data to the literature reports for all the products in synthetic steps. Quinoline core (**3**) and low molecular weight model compound (MQ) were prepared by Friedländer reaction between bis(aminoketone) (**1**) and 2 equiv of OH-substituted ketomethylene (**2-X**) in a manner similar to the literature.[16,27,28] The dendritic product QG*n* were prepared by coupling reactions between **3** and G*n*-Br by a standard method in the presence of anhydrous K_2CO_3 and 18-crown-6. As shown in Scheme 1, quinoline core **3** has four hydroxy groups capable of participating in the coupling reaction, i.e., two inner ones adjacent to quinoline ring and two outer ones opposite to it. The inner one is known to form intramolecular cyclic H-bond with nitrogen atom of quinoline and thus to show low nucleophilicity.[29] Hence, it can be assumed that the coupling reaction would selectively provide peripheral disubstitution of G*n*-Br at the outer hydroxy groups of **3**. In the case of the first generation, however, a considerable amount of trisubstitution as well as disubstitution occurred during the coupling reaction between **3** and G1-Br, as was detected by thin-layer chromatography and the MALDI-TOF mass spectrum of the crude product. The di- and trisubstituted products (QG1 and QG1-t) were isolated successfully by silica gel column chromatography with the yields of 28% and 19%, respectively. This result indicates that the intramolecular H-bond of **3** in solution is not strong enough to give a selective peripheral substitution. On going to the higher generation, trisubstitution became negligible due to the steric hindrance arising from the bulkiness of benzyl bromide dendron. Accordingly, the yield of the disubstituted product could be increased to 59% for QG2 and 77% for QG3.

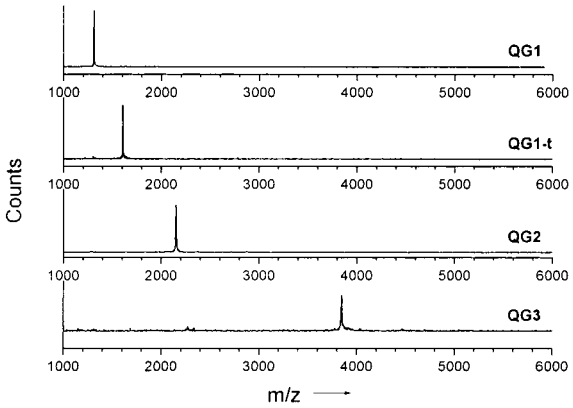

Figure 1. MALDI-TOF mass spectra of QG*n*.

All the isolated dendritic compounds by silica gel column chromatography showed acceptable purity and comparable mass to the theoretical value, as determined by MALDI-TOF spectra (Figure 1). It must be noted, however, that different isomers other than peripherally substituted ones are not distinguished by the chromatography and mass spectra. Careful examination of the IR spectra in Figure 2 was useful for this purpose, which strongly supported the peripheral substitution for all the isolated compounds. By comparing the IR spectra of **3** and MQ, we can assign the peak of inner hydroxy group from that of the outer one. The inner hydroxy peak of MQ is a weak and broad one centered at 3405 cm^{-1} due to the intramolecular H-bond, while the outer one of **3** exhibits a relatively sharp peak with middle intensity centered at 3360 cm^{-1}. Accordingly, it can be mentioned that all the isolated dendritic compounds showing hydroxy peak at ca. 3405 cm^{-1} (Figure 2) are isomers with peripheral substitutions. All the dendritic compounds QG*n* are amorphous glass and well soluble in common organic solvents. It is also noted that glass transition temperatures (T_g) tend to decrease from 105 to 50 °C with increasing dendrimer generation.

Static Optical Properties. The effect of dendritic framework on the optical properties of quinoline-based ESIPT core was investigated by electronic absorption and emission spectra. Figure 3a shows the absorption spectra of MQ and QG*n* in $CHCl_3$ solution, all of which comprise four main absorption bands. The poly(aryl ether) structure of dendron is known to have no electronic effect on core chromophore.[24] Furthermore, in our previous report, it was elucidated by quantum chemical calculation for isolated gas phase that the conjugation

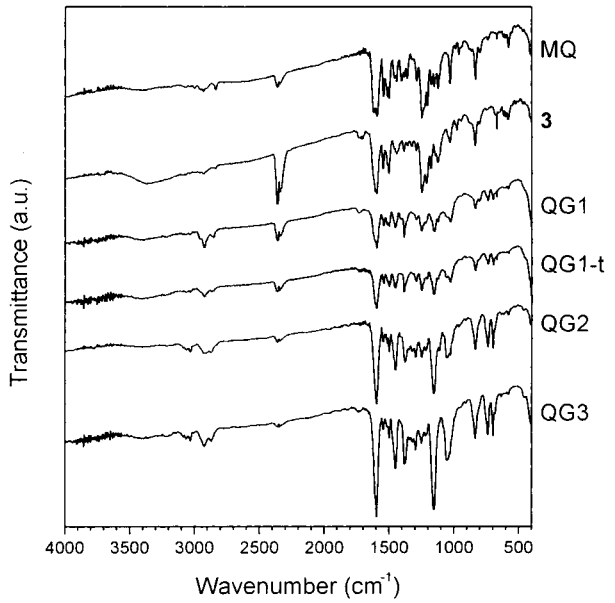

Figure 2. IR spectra of the quinoline-based low molar mass compounds (MQ, 3) and dendritic compounds QG*n*.

between quinoline and pendant phenyl ring attached at its 4-position is broken owing to a large torsional angle of ca. 67°.[16] This theoretical consideration is confirmed by the reported value of 49° in single cystals of similar quinoline compounds.[30] Thus, it can be mentioned that the π-conjugated unit in the ESIPT core is the 2-quinolin-2-yl-phenol moiety. From this consideration, two large energy bands below 300 nm can be assigned as transitions of poly(aryl ether) structure and pendant methoxyphenyl substituent in the core unit. The other two bands at ca. 378 nm and ca. 322 nm would be from the transition of conjugated core unit, each denoted as S1 and S2, respectively. As shown in the inset of Figure 3a, it is remarkable that the wavelength at absorption maximum (λ_{max}) of S1 and the absorbance ratio of S1 and S2 changes slightly but meaningfully with a tendency depending on the dendrimer generation, except for the trisubstituted QG1-t (denoted as open symbols). Since the increment of dendron generation means the growth of peripheral steric hindrance without electronic interaction with core, this spectral change may arise from the different planarity of conjugated core unit governed by the peripheral crowdedness. This assumption can be rationalized by the weak H-bond of the core chromophore in solution or the low rigidity of core plane, as discussed above. To be convinced of this idea, a semiempirical molecular orbital calculation with the simplified model structure shown in Figure 3b was carried out. The optimized geometry of model structure preferred the H-bonded conformation with perfect coplanarity between quinoline and phenol units ($\theta = 0$ in Figure 3b) and gave the calculated transition energies comparable to S1 and S2. Informatively, the larger energy band S2 is well accordant with the calculated transition energy of 6-methoxyquinoline (334 nm), implying that S2 is mainly from the quinoline segment. As the conjugation plane was distorted by increasing the torsional angle (θ) around the bond connecting quinoline and phenol units, the calculated contribution of S2 showed growth over that of S1. In other words, on going to a more planar conformation, the calculated tendency for the transition energy of S1 along with the oscillator strength

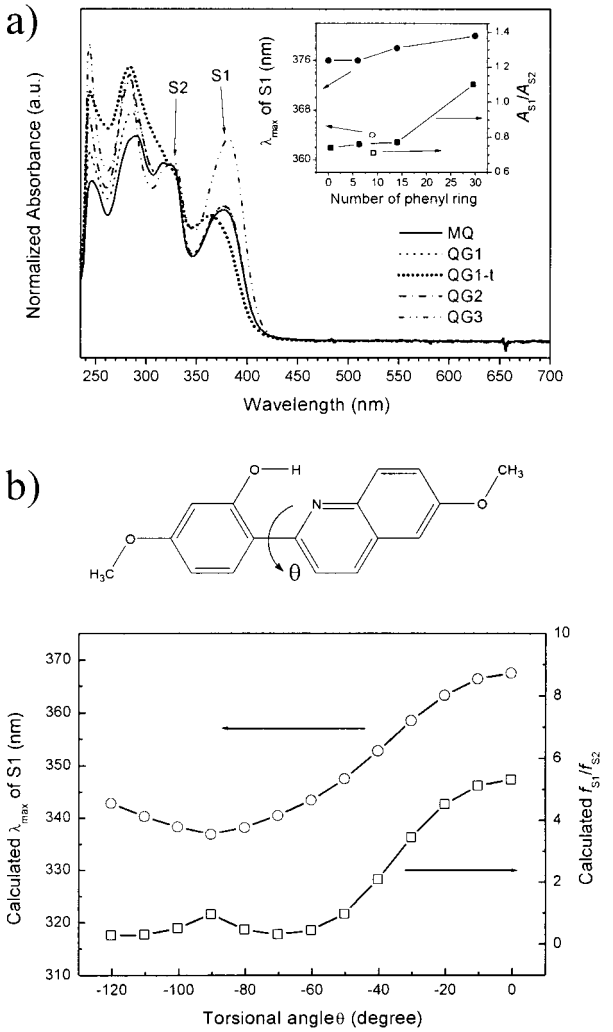

Figure 3. (a) Solution absorption spectra of MQ and QG*n* in $CHCl_3$ (10^{-5} M). The inset shows the tendency for λ_{max} of S1 band and the absorbance ratio of S1 and S2 bands as a function of the number of phenyl rings in dendron substituent (MQ, 0; QG1, 6; QG1-t, 9; QG2, 14; QG3, 30). (b) Simplified model structure for ESIPT chromophore and its planarity-dependent tendency for the calculated λ_{max} of S1 band and the oscillator strength (*f*) ratio of S1 and S2 bands. The planarity was distorted by changing θ by 10°.

(*f*) ratio of S1 and S2 is well consistent with the experimental observation on increasing the generation from MQ to QG3, as plotted in Figure 3. This calculation result demonstrates that in the case of peripherally disubstituted compounds the more sterically hindered periphery of the higher generation gives rise to the more planar core conformation in solution state. The deviation of trisubstituted QG1-t from the above tendency of disubstituted QG*n*'s can also be explained in the sense of core planarity. The central steric hindrance from a bulky dendritic substituent at the inner hydroxy group would strongly distort the core plane and disturb the conjugation, to result in the large hypsochromic shift relative to other compounds.

Except for crystalline MQ, all dendritic compounds QG*n* are glassy and formed a scattering-free transparent film when spin-coated. Figure 4 shows the absorption spectra of QG*n* films that display spectral characteristics similar to the solution absorption. Trisubstituted QG1-t showed hypsochromically shifted S1 also in the film state, indicating that the central steric hindrance is still significant in the condensed phase. For all

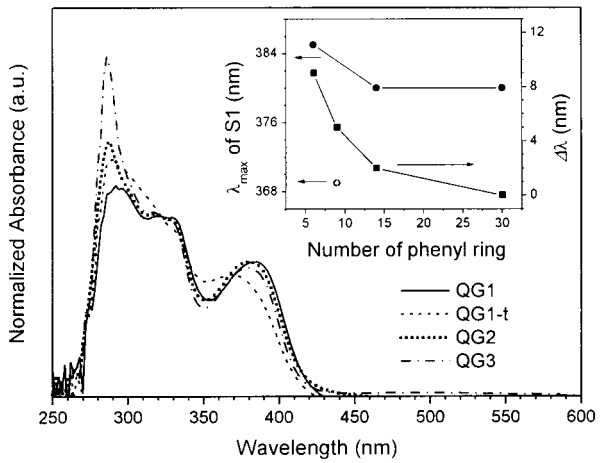

Figure 4. Film absorption spectra of QG*n*. The inset shows the tendency for λ_{max} of S1 band and its bathochromic shift ($\Delta\lambda$) relative to the solution absorption as a function of the number of phenyl rings in dendron substituent (defined in Figure 3).

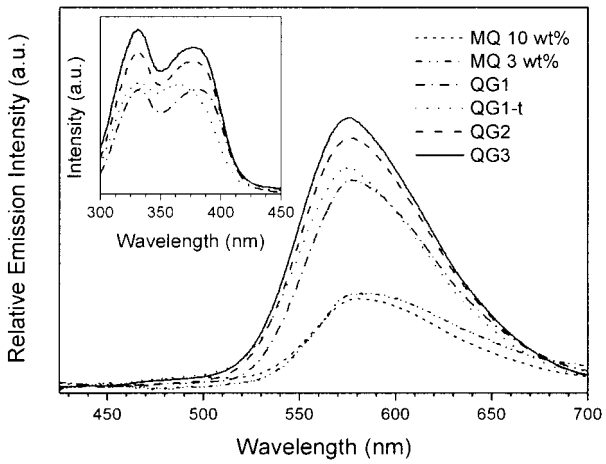

Figure 5. Relative emission intensities of QG*n* films and MQ−polystyrene blend films (3, 10 wt %), each spectrum obtained by excitation at 370 nm. The inset is the excitation spectra for the emission of QG*n* at 580 nm.

compounds except QG3, the λ_{max} values of S1 in film were bathochromically shifted relative to that in solution. The aggregation effect can be disregarded because no aggregation and no excimeric behavior were observed for this quinoline-based ESIPT chromophore even in the more concentrated film of PQH.[16] Thus, this spectral difference between solution and film is most probably attributed to the different core planarity between the two molecular states. This means that the core plane with low rigidity is affected not only by the intramolecular peripheral crowdedness but also by the intermolecular steric effect. Importantly, the bathochromic shift is the largest for QG1 that possesses the least hindered periphery and shows a tendency to decrease with increasing generation, i.e., increasing peripheral hindrance. This generation dependency in S1 λ_{max} is thus opposite to that in solution, as shown in the inset of Figure 4. Resultantly, on going to the higher generation, the core planarity in film is less different from that in solution such that eventually in the third generation dendrimer QG3 S1 λ_{max} is the same in both states. Here we note that solution and film are extreme cases of molecular states with different molecular surroundings, where the former is a solvated state with a large amount of kinetic freedom but the latter has kinetic constraint due to the intermolecular proximity. This spectral tendency thus means that the crowded periphery of dendritic shell not only determines the core planarity intrinsically but also decouples it from the molecular surroundings, forming a solid solution in the geometrical and spectral senses.

The generation effect on the emission behavior was studied for the film samples of QG*n*. As shown in Figure 5, all the QG*n* films emitted abnormally large Stokes shifted (∼200 nm) orange fluorescence without spectral overlap between absorption and emission. From the comparison with PQH of similar structure, it is unambiguous that this orange emission is attributed to the characteristic fluorescence from the proton-transferred excited keto form of quinoline-based core.[16] As reported in our previous work,[16] PQH solution gave dual emission from both enol and keto forms (ca. 400 and 590 nm, respectively) while the film gave only keto emission because the excited-state intramolecular proton transfer (ESIPT) in film was much faster than in solution by effective H-bond due to the suppressed molecular motion. Similar to PQH film, QG*n* films emitted no detectable fluorescence from the enol form in 360−500 nm, suggesting that the effective H-bond and the fast proton transfer are operating also in QG*n* films. Importantly, the relative emission intensity of QG*n* films, which was normalized by the absorbance at excitation wavelength of 370 nm, was increased with increasing number of phenyl rings in dendron shell, indicative of the improved efficiency of keto emission by the enhanced shell effect. Moreover, all the dendritic compounds QG*n*, whose chromophore content in total weight is from 18 wt % (QG3) to 54 wt % (QG1), showed dramatically enhanced emission intensity relative to that of nondendritic MQ in more dilute solid solution (3 and 10 wt % in polystyrene blend film). Thus, it can be concluded that the dendritic architecture shows enhanced performance for the "solid solution" with high chromophore content as well as improved emission efficiency. This is primarily due to the cooperative effect of dendritic shell that can actually separate the emitting core from each other to suppress the fluorescence quenching via molecular association.

Contrary to the film, the QG*n* solution shows no detectable emission from either the keto or enol form. It is not the case for PQH solution, giving dual emission. One possible explanation for this fluorescence quenching in solution can be given in the sense of twisted intramolecular charge transfer (TICT) state connected with a large-amplitude torsional vibration of core plane around the average planarity, which has been discussed in the literature for the similar ESIPT system of 3-hydroxy- and 3,3′-dihydroxy-2,2′-bipyridyl.[8] In the case of PQH, this quenching motion in solution might be constrained to some extent due to the reduced degree of freedom along the polymer backbone.

The excitation spectra for keto emission from QG*n* films are very similar to the absorption bands, S1 and S2, of the conjugated core, as shown in the inset of Figure 5. It is noted that the absorption of dendron shell below 300 nm has no contribution to fluorescence. Moreover, since the absorption is from the ground state mainly existing in enol form, its good accordance with the keto excitation strongly supports that the precursor of the excited keto form is the Franck−Condon excited state of enol form.

Fluorescence Kinetics. Figure 6 shows the picosecond kinetic profiles of the emission above 550 nm

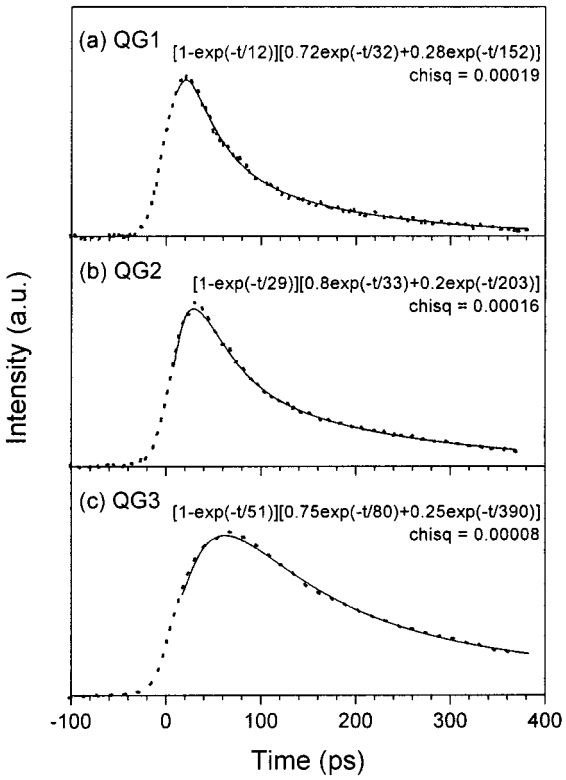

Figure 6. Fluorescence kinetic profiles (dotted) of QG*n* emission above 550 nm, each plotted with the best-fitted kinetic functions (solid).

from QG*n* films. The best-fitted kinetic functions are all composed of single-exponential rise and double-exponential decay. The delayed rise of picosecond scale is attributable to the proton transfer from the Franck−Condon excited state of enol form upon excitation and provides direct evidence that the orange emission of QG*n* films is the fluorescence from the excited keto form following ESIPT, rather than phosphorescence from the excited enol form. On increasing the generation, the fluorescence rise is slowed down with the time constant from 12 to 51 ps due to the reduced planarity of core in the film state. It is considered that the effective H-bond and fast ESIPT are more achievable in the more planar conformation. Nevertheless, the absence of blue enol emission in all the QG*n* films strongly suggests that ESIPT is still so effective even in higher generation that the excited enol form decays mainly to the excited keto form by proton transfer rather than radiatively to the ground-state enol form.

The biphasic decay of keto emission implies an additional photochemical process in the excited proton-transferred state beside radiative decay. As discussed in our previous study,[16] the fast decay with the lifetime of 32−80 ps can be assigned as the electronic rearrangement from the excited zwitterionic form, which is formed just after ESIPT, to the excited keto form. Electronic rearrangement is known to follow fast proton transfer to form relatively more stable species in the S_1 states of quinoline derivatives.[31,32] The slow decay is attributable to the radiative decay of the excited keto form. The lifetime of the slow decay tended to increase from 152 to 390 ps with increasing generation. This observation correlates well with the increase in fluorescence efficiency and therefore supports the enhanced relative emission intensity with increasing generation shown in the static spectra (Figure 5).

Conclusions

Poly(aryl ether)-type dendrimers cored with ESIPT-active quinoline were synthesized and identified. It was founded that the dendritic shells are able to decouple the core planarity from the molecular surroundings and to enhance ESIPT emission by the spatial isolation of ESIPT cores. It was demonstrated for the first time that the ESIPT dendrimers are a new class of solid ESIPT medium with large content of active chromophores and efficient ESIPT emission.

Acknowledgment. This research was supported in part by CRM-KOSEF.

References and Notes

(1) McMorrow, D. C.; Kasha, M. *J. Phys. Chem.* **1984**, *88*, 2235.
(2) *Chem. Phys.* **1989**, *136*; special issue on proton-transfer reactions.
(3) Grabowska, A.; Sepiol, J.; Rullière, C. *J. Phys. Chem.* **1991**, *95*, 10493.
(4) Arnault, L. G.; Formosinho, S. J. *J. Photochem. Photobiol. A: Chem.* **1993**, *75*, 1.
(5) Roberts, E. L.; Chou, P. T.; Alexander, T. A.; Agbaria, R. A.; Warner, I. M. *J. Phys. Chem.* **1995**, *99*, 5431.
(6) Chou, P. T.; Chen, Y. C.; Yu, W. S.; Chou, Y. H.; Wei, C. Y.; Cheng, Y. M. *J. Phys. Chem.* **2001**, *105*, 1731.
(7) Foster, K. L.; Baker, S.; Brousmiche, D. W.; Wan, P. *J. Photochem. Photobiol. A: Chem.* **1999**, *129*, 157.
(8) Vollmer, F.; Rettig, W. *J. Photochem. Photobiol. A: Chem.* **1996**, *95*, 143.
(9) Acuña, A. U.; Amat-Guerri, F.; Costela, A.; Douhal, A.; Figuera, J. M.; Florido, F.; Sastre, R. *Chem. Phys. Lett.* **1991**, *187*, 98.
(10) Formosinho, S. J.; Arnault, L. G. *J. Photochem. Photobiol. A: Chem.* **1993**, *75*, 21.
(11) Tarkka, R. M.; Zhang, X.; Jenekhe, S. A. *J. Am. Chem. Soc.* **1996**, *118*, 9438.
(12) Costela, A.; García-Moreno, I.; Mallavia, R.; Amat-Guerri, F.; Barroso, J.; Sastre, R. *Opt. Commun.* **1998**, *152*, 89.
(13) LeGourriérec, D.; Kharlanov, V.; Brown, R. G.; Rettig, W. *J. Photochem. Photobiol. A: Chem.* **1998**, *117*, 209.
(14) Tarkka, R. M.; Jenekhe, S. A. *Chem. Phys. Lett.* **1996**, *260*, 533.
(15) Campo, L. F.; Corrêa, D. S.; de Araújo, M. A.; Stefani, V. *Macromol. Rapid Commun.* **2000**, *21*, 832.
(16) Chang, D. W.; Kim, S.; Park, S. Y.; Yu, H.; Jang, D.-J. *Macromolecules* **2000**, *33*, 7223.
(17) Jin, R.-H.; Aida, T.; Inoue, S. *J. Chem. Soc., Chem. Commun.* **1993**, 1260.
(18) Dandliker, P. J.; Diederich, F.; Gross, M.; Knobler, C. B.; Louati, A.; Sanford, E. M. *Angew. Chem., Int. Ed. Engl.* **1994**, *33*, 1739.
(19) Dandliker, P. J.; Diederich, F.; Gisselbrecht, J.-P.; Louati, A.; Gross, M. *Angew. Chem., Int. Ed. Engl.* **1995**, *34*, 2725.
(20) Jiang, D.-L.; Aida, T. *Chem. Commun.* **1996**, 1523.
(21) Bar-Haim, A.; Klafter, J.; Kopelman, R. *J. Am. Chem. Soc.* **1997**, *119*, 6197.
(22) Jiang, D.-L.; Aida, T. *Nature (London)* **1997**, *388*, 454.
(23) McKeown, N. B. *Adv. Mater.* **1999**, *11*, 67.
(24) Gilat, S. L.; Adronov, A.; Fréchet, J. M. J. *Angew. Chem., Int. Ed.* . **1999**, *38*, 1422.
(25) Hawker, C. J.; Fréchet, J. M. J. *J. Am. Chem. Soc.* **1990**, *112*, 7638.
(26) Riley, J. M.; Alkan, S.; Chen, A.; Shapiro, M.; Khan, W. A.; Murphy, Jr., W. R.; Hanson, J. E. *Macromolecules* **2001**, *34*, 1797.
(27) Agrawal, A. K.; Jenekhe, S. A. *Macromolecules* **1993**, *26*, 895.
(28) Zhang, X.; Shetty, A. S.; Jenekhe, S. A. *Macromolecules* **1999**, *32*, 7422.
(29) Ma, H.; Wang, X.; Wu, X.; Liu, S.; Jen, A. K.-Y. *Macromolecules* **1998**, *31*, 4049.
(30) Shetty, A. S.; Liu, E. B.; Lachicotte, R. J.; Jenekhe, S. A. *Chem. Mater.* **1999**, *11*, 2292.
(31) Bardez, E.; Chatelain, A.; Larrey, B.; Valeur, B. *J. Phys. Chem.* **1994**, *98*, 2357.
(32) Bardez, E.; Fedorov, A.; Berberan-Santos, M. N.; Martinho, J. M. G. *J. Phys. Chem. A* **1999**, *103*, 4131.

MA011385O